IEEE Open Journal of
Intelligent Transportation
Systems

Received 4 January 2022; revised 14 July 2022, 18 January 2023, and 18 February 2023; accepted 20 February 2023. Date of publication 9 March 2023; date of current version 31 March 2023.

Digital Object Identifier 10.1109/OJITS.2023.3254886

On the Characterization of Eco-Friendly Paths for Regional Networks

SÉRGIO F. A. BATISTA [1], MOSTAFA AMELI [2,3], AND MÓNICA MENÉNDEZ [1] (Member, IEEE)

[1]Division of Engineering, New York University Abu Dhabi, Abu Dhabi, UAE

[2]COSYS, GRETTIA, Université Gustave Eiffel, 77420 Champs-sur-Marne, France

[3]Department of Electrical Engineering and Computer Sciences, University of California at Berkeley, Berkeley, CA 94720, USA

CORRESPONDING AUTHOR: S. F. A. BATISTA (e-mail: sergio.batista@nyu.edu)

The work of Sérgio F. A. Batista and Mónica Menéndez was supported by the NYUAD Center for Interacting Urban Networks (CITIES) and by the NYUAD Arabian Center for Climate and Environmental Sciences (ACCESS), funded by Tamkeen under the NYUAD Research Institute Award CG001 and the NYUAD Research Institute Award CG009, respectively.

ABSTRACT Macroscopic traffic models represent a promising tool to design strategies for ecological routing. To benefit from this tool, we must first characterize the relationship between path emissions and distance traveled or travel time on aggregated networks, i.e., a regional network. This paper investigates this relationship between two toy networks and a real urban network representing the city of Innsbruck (Austria). We utilize an accumulation-based model based on the Macroscopic Fundamental Diagram to mimic the traffic dynamics in the network and utilize the COPERT IV model to estimate the travel emissions, focusing on the carbon dioxide CO_2. We show that there is a linear relationship between the total emissions of CO_2 and the average travel time of internal paths, i.e., paths that take place completely within a single region. We also show that in some cases, there is a linear relationship between the total emissions and the average travel distance or travel time of paths that cross multiple regions in the network. However, the latter is not always true as traffic dynamics play an important role in path emissions. In other words, eco-friendly paths on regional networks do not necessarily follow the shortest paths in terms of distance or time.

INDEX TERMS Eco-friendly paths, regional networks, macroscopic fundamental diagram, travel time, travel distance.

I. INTRODUCTION

ROAD transportation has a non-negligible effect on the emission of atmospheric pollutants of carbon dioxide CO_2. Carbon dioxide is responsible for the increase of the greenhouse effect and, therefore, global warming. Hence, there is a need for designing innovative strategies to help mitigate traffic emissions. One example is the deployment of sustainable transportation policies, like low-emission zones. Another example relies on traffic management strategies through the concept of green routing, where drivers choose routes that minimize energy and/or fuel consumption and therefore exhaust emissions. This concept was early introduced by [1]. Many scholars have studied and designed various green-routing models where traffic emission costs are incorporated ([2], [3], [4], [5], [6], [7], [8], [9], [10], [11], [12], [13], [14], [15], [16]). These models have had limited applicability due to the large computational power and time required for running dynamic traffic simulations in large metropolitan areas. The aggregated traffic models based on the Macroscopic Fundamental Diagram (MFD) [17] present promising prospects in this regard [18], [19]. However, the application of MFD-based models for studying and monitoring exhaust emissions resulting from traffic is still an underdeveloped field of research.

One of the key elements in the development of efficient green-routing strategies is understanding the relationship

The review of this article was arranged by Associate Editor Margarida Coelho.

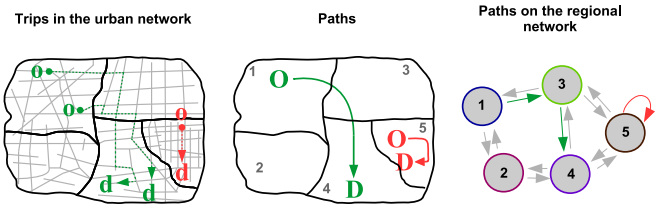

FIGURE 1. Example of trips in the urban network, and their corresponding paths on the regional network. Source: [28].

between travel distance or travel time of routes and the total exhaust emissions. The question is how to design efficient incentive policies to make drivers choose routes that are potentially longer than the shortest one in distance or time for their journey, but that are also ecologically friendlier (i.e., eco-friendly). Interestingly, several seminal works ([13], [20], [21], [22]) showed that choosing eco-friendly routes can come at the expense of longer travel times for drivers. Intuitively, one might think that the shortest path or fastest path would also be the most environmentally friendly. However, there is still some debate in the literature about this question. Some scholars have pointed out that routes with minimal travel times also often minimize energy consumption and emissions ([23], [24], [25]). Other studies ([9], [13], [20], [26], [27]) have demonstrated that the shortest paths in distance or the fastest paths might not necessarily be the most environmentally friendly. The shortest paths in distance might be highly congested, where the stop-and-go waves become more frequent, resulting in an increase in exhaust emissions. On the other hand, the fastest paths are usually associated with highways, leading drivers to take long detours to avoid the congested areas in the city.

The characterization of eco-friendly paths becomes more complex in the case of MFD-based traffic models. This is because the definition of the path for this kind of aggregated model is different from the one of trips in urban networks [28] (see Figure 1). The application of the MFD-based models requires the aggregation of the urban network into a set of regions ([29], [30]), within which vehicles circulate at the same average speed. This enables the definition of a regional graph (or regional network). The nodes of this graph represent the regions. The links between adjacent regions depend on the urban network topology, i.e., on the allowed travel directions in the urban network between adjacent regions. Figure 1 depicts the difference between trips in the urban network and paths on the regional network. From the origin (o) to the destination (d) nodes, the ordered sequence of traveled links defines a trip in the urban network. These trips are also characterized by a fixed physical length [31]. Reference [28] defines a path on the regional network as an ordered sequence of traveled regions from the Origin (O) to the Destination (D) regions. As depicted in Figure 1, both green trips cross the same sequence of regions following the definition of network partitioning. This means that they are associated with the same path on the regional network, even though each of these trips travels a different distance inside each region, and has a different origin (o) and destination (d) node within the Origin (O) and Destination (D) regions, respectively. This leads to an explicit distribution of travel distances [32] that characterizes each region of each path in the regional network.

Using a simulation-based approach, this paper investigates the relationship between the average travel distance or travel time and the level of total exhaust emissions of paths on regional networks. Understanding this relationship is important for deploying appropriate network-wide optimal eco-routing strategies using the MFD dynamics. There are three important key aspects that might play a role in the characterization of eco-friendly paths in regional networks:

- the speed homogeneity assumption of the MFD, i.e., all vehicles travel at the same mean speed in any given region independently of their path;
- the heterogeneity of travel distances in each region that results from all paths that cross this region; and
- the interactions between different OD pairs.

Therefore, we analyze the existence of the relationship between travel exhaust emissions and travel distance and/or travel time. To that end, we first focus on a 1-region network with multiple paths. In such a case, we consider that all paths are internal, i.e., they take place completely within a single region. Second, we calculate the Deterministic User Equilibrium (UE) [33] and Deterministic Bounded Rational User Equilibrium (BR-UE) on a 4-region network, considering a scenario with a single OD pair and another one with 2 OD pairs. Third, we apply the previous equilibrium conditions to a real urban network representing the city of Innsbruck (Austria), partitioned into 4 regions. Note that, we consider in our experiments the calculation of the Deterministic User Equilibrium and the Bounded Rational User Equilibrium so that we can cover different network loading conditions for the demand profiles we considered in each scenario. Evidently, it would also be possible to only consider fixed path assignments in our analysis. However, by considering the dynamic network equilibria, we account for drivers switching paths dynamically when travel distances increase or when they perceive congestion in the network. In this analysis, we utilize an accumulation-based MFD model [34] to mimic the traffic dynamics on these regional networks and the aggregated COPERT IV [35] model to estimate the regions' emissions. We focus on the carbon dioxide CO_2 emissions in this study. However, we expect the findings to be relevant for the estimation of other types of emissions as well.

The remainder of the paper is organized as follows. Section II describes the formulation and solution algorithm for the calculation of the Deterministic User Equilibrium and Bounded Rational User Equilibrium on regional networks. Section III introduces the COPERT IV emission model. Section IV analyzes the relationship between the travel distance and travel time and the total exhaust emissions along

paths on regional networks, under different scenarios, and on small toy networks. Section V analyses the same relationship but on a real urban network representing the city of Innsbruck (Austria). Section VI outlines the main conclusions of this paper.

II. DYNAMIC USER EQUILIBRIUM ON REGIONAL NETWORKS

This section presents the mathematical formulation and solution algorithm for calculating the Dynamic Deterministic User Equilibrium and Dynamic Bounded Rational User Equilibrium on regional networks.

A. DETERMINISTIC USER EQUILIBRIUM

As discussed in the Introduction, paths on regional networks are characterized by an explicit distribution of travel distances. Such distributions can be estimated using the methodology proposed by [32]. Using these explicit distributions of travel distances, [36] defines the travel time of a path p, TT_p^{OD}, on a regional network as:

$$TT_p^{OD} = \sum_{r \in X} \frac{L_{rp}}{v_r(n_r(t))} \cdot \delta_{rp}, \forall (O, D) \in W \tag{1}$$

where W denotes the set of all regional OD pairs; n_r is the accumulation of region r; and δ_{rp} is a binary variable that equals 1 if path p goes through region r, and 0 otherwise; L_{rp} denotes the explicit distribution of travel distances in region r of path p; v_r is the distribution of mean-speeds in region r; X denotes the set of all regions within the regional network; and t represents the simulation time. For ease of notation, in the equations that follow, we omit the dependence of the accumulation n_r and mean speeds $\bar{v}_r$ on t. Note that, the total average travel distance of a path p, $\bar{L}_p$, is determined as $\bar{L}_p = \sum_{r \in X} \bar{L}_{rp} \cdot \delta_{rp}$, where $\bar{L}_{rp}$ represents the average travel distance of path p in the region r.

Based on Eq. (1), [36] approximates the path travel times TT_p^{OD} by calculating the first-order Taylor series expansion around the average value of the explicit distributions of travel distances ($\bar{L}_{rp}$) and the mean speed ($\bar{v}_r(n_r)$). In the Deterministic User Equilibrium, none of the terms are considered to be distributed, and Eq. (1) becomes:

$$\overline{TT}_p^{OD} = \sum_{r \in X} \frac{\bar{L}_{rp}}{\bar{v}_r(n_r)} \cdot \delta_{rp}, \forall (O, D) \in W \tag{2}$$

where $\bar{v}_r(n_r)$ represents the spatial average of the mean speed over a time interval.

In this paper, we assume that under the Deterministic User Equilibrium conditions, drivers aim to minimize their own travel times as given by Eq. (2).

B. BOUNDED RATIONAL USER EQUILIBRIUM

The idea of bounded rationality was initially introduced by [37] and later adapted to the route choice context by [38]. The bounded rationality of drivers arises from habits or preferences for their route choices. This concept relaxes the travel time minimization assumption of the Deterministic User Equilibrium [39]. Instead, drivers choose *satisficing* routes, i.e., routes that have a perceived travel time shorter than a pre-defined threshold or aspiration level (see, e.g., [39], [40]). The term *satisficing* introduced by [37] comes from the combination of the words "suffice" and "satisfy". Reference [41] was the first to apply the bounded rational behavior for path choices on regional networks considering the MFD dynamics. Under the bounded rational behavioral assumption, drivers choose paths that satisfy the following condition:

$$\overline{TT}_p^{OD} \leq AL^{OD}, \forall (O, D) \in W \tag{3}$$

where AL^{OD} represents the Aspiration Level for the regional OD pair. Note that all drivers traveling on the same OD pair have the same AL^{OD}.

The aspiration AL^{OD} is determined based on the indifference band Δ^{OD} [38] as:

$$AL^{OD} = \min\left(\vec{TT}^{OD}\right)\left(1 + \Delta^{OD}\right), \forall (O, D) \in W \tag{4}$$

where $\vec{TT}_p^{OD}$ is a vector that contains all the values of the average travel times $\overline{TT}_p^{OD}$ of all paths connecting the OD pair; and $\Delta^{OD} \in [0, +\infty)$ is the indifference band that is exogenously defined. Note that when $\Delta^{OD} = 0$, the Bounded Rational User Equilibrium is equivalent to the classical Deterministic User Equilibrium.

In this paper, we also consider that drivers have an indifference preference for their path choices based on [41], which means that the demand is equally split over all paths that are perceived as *satisficing*.

C. SOLUTION ALGORITHM

In this paper, we utilize the classical Method of Successive Averages to determine the network equilibrium, with a descent step of $1/j$ and where j denotes the descent step iteration. As stopping criteria [41], we utilize the Gap function, the number of violations $N(\phi)$ or a maximum number of descent step iterations (N^{max}). The number of violations indicates how many paths per OD pair have the difference between the path flows of two consecutive descent steps, superior to the pre-defined threshold *Phi*. The convergence is achieved when $N(\phi) \leq Phi$. The Gap function monitors how far a given set of travel times is from the network equilibrium conditions [42]. In the case of the Deterministic User Equilibrium, the Gap is:

$$Gap^{UE} = \frac{\sum_O \sum_D \sum_{p \in \Omega^{OD}} Q_p^{OD}\left(\vec{TT}_p^{OD} - \min\left(\vec{TT}^{OD}\right)\right)}{\sum_O \sum_D Q^{OD} \min\left(\vec{TT}^{OD}\right)} \tag{5}$$

where Q^{OD} denotes the total demand for the OD pair; $Q_p^{OD} \in [0, 1]$ represents the path assignment coefficient; and Ω^{OD} denotes the regional choice set that lists all paths connecting the OD pair. Note that, under perfect Deterministic User Equilibrium conditions, the Gap^{UE} equals 0.

In the case of the Bounded Rational User Equilibrium, the Gap is:

$$Gap^{BR} = \frac{\sum_O \sum_D \sum_{p \in \Omega^{OD}} Q_p^{OD} \cdot \max\left(\overrightarrow{U}^{OD} - AL^{OD}, 0\right)}{\sum_O \sum_D Q^{OD} \cdot AL^{OD}} \tag{6}$$

where $\overrightarrow{U}^{OD}$ is a vector that contains all utility values of all paths that connect the same OD pair.

We determine the network equilibrium using a quasi-static approximation, where the total simulation period T is split into smaller intervals of duration $\delta t = 6$ [min]. We calculate the network equilibrium for each of these time intervals. The path flows are maintained constant during each time interval. This quasi-static approximation permits us to account for changes within the traffic dynamics in the regions and the evolution of the demand.

III. COPERT EMISSION MODEL

In this paper, we utilize the COPERT IV [35] aggregated emission model to estimate the regions' emissions using the MFD dynamics. The COPERT IV model is a suitable choice for this study since it is applicable to a neighborhood or a small region (see, e.g., [43], [44]). Moreover, this model estimates the total exhaust emissions based on mean speeds $\overline{v}_r$ and aggregated travel distances per neighborhood, which we approximate by the travel production P_r. The MFD-based models yield these two variables.

The total exhaust emissions $E_{p,y}$, during a given time interval δt, of a given pollutant y are determined as:

$$E_{p,y} = \sum_{r \in X} EF_{r,y}(\overline{v}_r) \times P_r(n_r, \overline{v}_r) \times \delta t, \forall r \in X \tag{7}$$

where $P_r(n_r, \overline{v}_r)$ denotes the travel production of region r; and $EF_{r,y}$ is the unitary emission factor of pollutant y and region r. Note that, we approximate the total distance traveled by all vehicles in the region r and during the time interval δt, by the travel production $P_r(n_r, \overline{v}_r)$. In this paper, we focus only on carbon dioxide, i.e., $y = CO_2$.

The unitary emission factor of pollutant y is a convex function of the region's mean speed $\overline{v}_r(n_r)$. These unitary emission factors are defined for each class of vehicles (i.e., private cars, trucks, etc.), but in this paper, we only focus on private cars. The unitary emission factors already account for the accelerations and decelerations of vehicles, i.e., driving cycles, for each mean speed value. Here, we consider the calibration of the unitary emission factors as discussed in [43]. For this calibration, [43] utilized reference emission data collected in intervals of $\delta t = 6$ [min], using dynamometers installed on a fleet of vehicles. This fleet consisted of 30% EURO 5 and 24% Euro 4 diesel vehicles, which represents the French urban fleet for the year 2015. Based on this data, [45] fitted a fourth-degree polynomial for the unitary emission factor of CO_2:

$$EF_{CO_2}(\overline{v}_r) = \beta_1 \overline{v}_r^4 + \beta_2 \overline{v}_r^3 + \beta_3 \overline{v}_r^2 + \beta_4 \overline{v}_r + \beta_5 \tag{8}$$

where $\beta_1 = 4.15 \times 10^{-6}$, $\beta_2 = -1.04 \times 10^{-3}$, $\beta_3 = 1.00 \times 10^{-1}$, $\beta_4 = -4.47$ and $\beta_5 = 123.54$ are the regression coefficients.

IV. CHARACTERIZATION OF ECO-FRIENDLY PATHS ON REGIONAL NETWORKS

This section analyzes the relationship between the total exhaust emissions of CO_2 along paths on regional networks and the travel distance and travel time. The numerical experiments are conducted on two regional toy networks composed of 1- and 4-region.

A. NETWORK SETTINGS AND SIMULATION SCENARIOS

This section describes the experimental design setup of our test scenarios. Figure 2 depicts the 1-region and 4-region networks. Traffic is modeled using an accumulation-based MFD model [34]. We consider a total simulation time of 3 [hr] for all simulations. We design six different scenarios:

Scenario 1: The single-region network depicted in Figure 2 (a) represents the test network, having 20 internal paths with different travel distances ranging from approximately 1 to 14 [kms]. Figure 3 (a) shows the demand traveling on each internal path. This demand profile is similar for all internal paths. Figure 3 (b) shows the production-MFD of this network. The MFD function has a maximum production of 30000 [veh.m/s], a critical accumulation of 4000 [veh], a jam accumulation of 10000 [veh], and a free-flow speed of 15 [m/s].

Scenario 2: Figure 2 (b) shows the second test network, which has four regions and a single OD pair: region 1 is the Origin, and region 4 is the Destination. There are two regional paths connecting this OD pair: $p_1 = \{124\}$ and $p_2 = \{134\}$. The average travel distances in all regions, except region 2, are equal to 1 [km]. The average travel distance of region 2 ranges between 0.1 and 3 [km], increasing step-wise by 0.1 [km]. Figure 3 (c) depicts the demand profile for the unique OD pair 14. In this scenario, we equally split the demand on both regional paths throughout the whole simulation period. We also consider a concave production-MFD function for all regions as depicted in Figure 3 (b), but with different parameters. The MFD function has a maximum production of 4000 [veh.m/s], a critical accumulation of 533 [veh], a jam accumulation of 3000 [veh], and a free-flow speed of 15 [m/s].

Scenario 3: This scenario is similar to the previous one, except that we determine the path flow distribution corresponding to the Deterministic User Equilibrium conditions as described in Section II. The network is under Deterministic User Equilibrium conditions when the Gap is inferior to a tolerance of 0.1. We also consider a maximum number of 20 descent-step iterations.

Scenario 4: This scenario is similar to the previous one plus an additional internal path in region 3, as depicted in Figure 2 (b). This internal path has an average travel distance of 1 [km]. Besides, we consider a constant demand of 1 [veh/s] for the whole simulation period for this path.

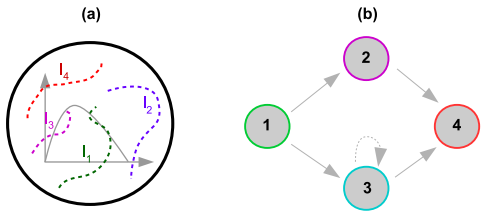

FIGURE 2. (a) 1-region network with several internal paths. (b) 4-region network.

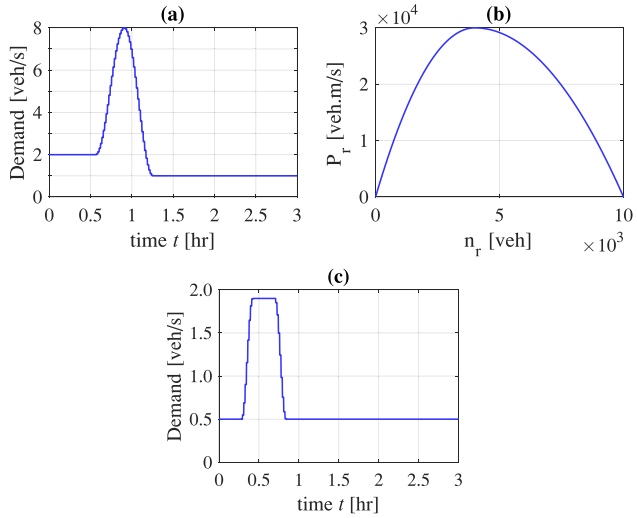

FIGURE 3. (a) Demand [veh/s] profile as a function of the simulation time t [hr], used for the 1-region network. (b) Production MFD is considered for all regions of both networks. (c) Demand [veh/s] profile as a function of the simulation time t [hr], used for the 4-region network.

Scenario 5: This scenario is similar to Scenario 3, but we determine the path flow distribution corresponding to the Bounded Rational User Equilibrium. We consider the following values of the indifference band Δ^{OD}: 0; 0.1; 0.2; and 1.0. Similar to Scenario 3, the network achieves the Bounded Rational User Equilibrium when the Gap is also inferior to a tolerance of 0.1.

Scenario 6: This scenario is similar to Scenario 4, but we determine the path flow distribution corresponding to the Bounded Rational User Equilibrium conditions as in the previous Scenario 5, and consider the same values for the indifference band Δ^{OD}.

B. 1-REGION NETWORK WITH SEVERAL INTERNAL PATHS

This subsection discusses the results for Scenario 1. Figure 4 depicts the total carbon dioxide emissions ($E_p(CO_2)$) as a function of the travel distance and travel time of all 20 internal paths in the 1-region network (Figure 2 (a)). As one can observe, there is a clear linear relationship between the level of CO_2 emissions and the average travel distance of a path as well as the average travel time. This happens because of the MFD assumption of homogeneous traffic conditions in the region, where all vehicles travel at the same average speed independently of their path. Since the

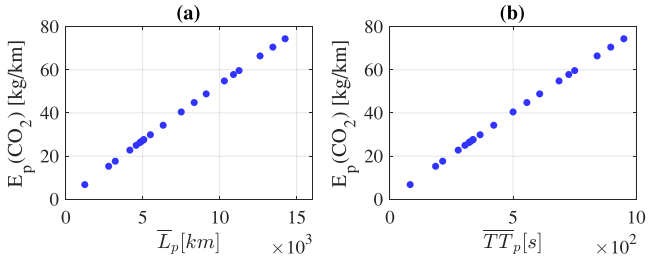

FIGURE 4. Total emissions of carbon dioxide ($E_p(CO_2)$) as a function of the internal paths (a) average travel distances $\overline{L}_p$ [km], and (b) average travel times $\overline{TT}_p$ [s]. The results correspond to Scenario 1.

average speed is the same for all vehicles, the average travel time $\overline{TT}_p$ is proportional to the average travel distance $\overline{L}_p$ of a path, i.e., $\overline{TT}_p \propto \overline{L}_p$. Therefore, vehicles traveling on longer internal paths also require more time to complete their trips. A longer average travel distance $\overline{L}_p$ also leads to a larger travel production P_r. This explains the linear relationship observed in Figure 4 also based on Eq. (7).

C. 4-REGION NETWORK WITH FIXED NETWORK LOADING

This subsection analyzes the results for Scenario 2, tested on the 4-region network (Figure 2 (b)). Figure 5 (a) depicts the path flows $Q_p, \forall p = 1, 2$ as a function of the average travel distance $\overline{L}_1$ [km] of path 1. Figure 5 (b) shows the total emissions of carbon dioxide ($E_p(CO_2), \forall p = 1, 2$) also as a function of the average travel distance $\overline{L}_1$ [km] of path 1.

In this scenario, the demand is equally assigned to paths $p_1 = \{124\}$ and $p_2 = \{134\}$, independently of their travel distance. One can observe that as the average travel distance $\overline{L}_1$ [km] of path 1 increases, the total emissions of carbon dioxide $E_1(CO_2)$ increase. The increase in the average travel distance in region 2 means that drivers require more time to complete their trips in this region. This increases the region's accumulation and reduces the mean speed $\overline{v}_2$, therefore leading to an increase in the total emissions of carbon dioxide CO_2 of the path $p_1 = \{124\}$. On the other hand, as the average travel distance of path 2 remains unchanged, the average travel time $\overline{TT}_2$ and the total emissions of carbon dioxide $E_2(CO_2)$ are constant (Figure 5 (c)). One can also observe that as the average travel distance $\overline{L}_1$ [km] of path 1 increases, the total network emissions $E(CO_2)$ also increase (Figure 5 (d)). Recall that both paths flow Q_p remain unaltered in this Scenario. The increase of $\overline{L}_1$ leads to an increase in the total distance traveled by vehicles in the network and therefore to the increase in the travel production, which in turn increases the accumulation in the network, reducing the mean speed $\overline{v}_r$. Based on Eq. (2), a larger travel production and a lower mean speed $\overline{v}_r$ lead to an increase of the total emissions of CO_2.

D. 4-REGION NETWORK UNDER UE CONDITIONS

This subsection analyzes the results for Scenarios 3 and 4, tested on the 4-region network (Figure 2 (b)). Figure 6 (a)

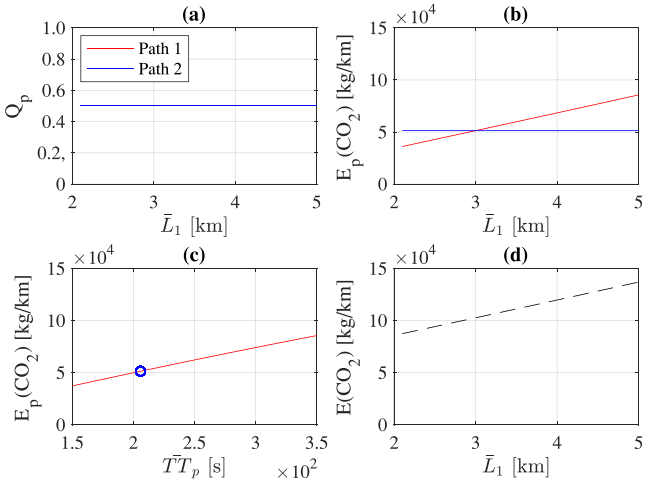

FIGURE 5. Path flows $Q_p, \forall p = 1, 2$ and total path emissions of carbon dioxide ($E_p(CO_2), \forall p = 1, 2$) as a function of the average travel distance $\bar{L}_1$ [km] of path 1. The path emissions of carbon dioxide ($E_p(CO_2), \forall p = 1, 2$) as a function of the average path travel times $\bar{TT}_p, \forall p = 1, 2$ [s], and the total network emissions of CO_2 ($E(CO_2)$) as a function of the average travel distance $\bar{L}_1$ [km] of path 1, are also depicted.

and (b) depict the path flows $Q_p, \forall p = 1, 2$ as a function of the average travel distance $\bar{L}_1$ [km] of path 1. Figure 6 (c) and (d) show the total emissions of carbon dioxide ($E_p(CO_2), \forall p = 1, 2$) also as a function of the average travel distance $\bar{L}_1$ [km] of path 1. Figure 6 (e) and (f) show the total emissions of carbon dioxide ($E_p(CO_2), \forall p = 1, 2$) as a function of the average path travel times $\bar{TT}_p, \forall p = 1, 2$ [s]. The first path is $p_1 = \{124\}$ and the second one is $p_2 = \{134\}$.

In Scenario 3, we calculated the User Equilibrium conditions of the network for all values of the average travel distances $\bar{L}_1$ [km] of path 1. Figure 6 (a), (c), (e) and (g) depict these results. We observe that for low values of $\bar{L}_1$, all drivers choose path 1, i.e., $p_1 = \{124\}$. As $\bar{L}_1$ increases, the total emissions of carbon dioxide $E_1(CO_2)$ also increase until some drivers start to switch to path 2, i.e., $p_2 = \{134\}$. Drivers start to switch to path 2 when the average travel time of this path becomes more attractive, leading to an increase of the total CO_2 emissions on this path and the consequent reduction on path 1. For larger values of $\bar{L}_1$, the average travel time of path 2 is shorter than that of path 1, and all drivers switch to path 2. As all the demand switches to path 2, the total emissions of CO_2 converge to a constant value as $\bar{L}_1$ increases. A similar trend is observed in the total emissions of CO_2 as a function of the path's average travel times. The total network emissions of CO_2 also increase as a function of $\bar{L}_1$ until $\bar{L}_1 \sim 3$ [km], i.e., until all drivers switch to path 2. The increase in the total emissions of CO_2 happens due to the increase in the travel production in the network, as in Scenario 2. When all drivers choose path 2, the total network emissions remain constant as $\bar{L}_1$ increases. This happens because, for this demand scenario, we do not observe congestion in the network.

In Scenario 4, we also target the User Equilibrium of the network for all values of $\bar{L}_1$. The difference concerning

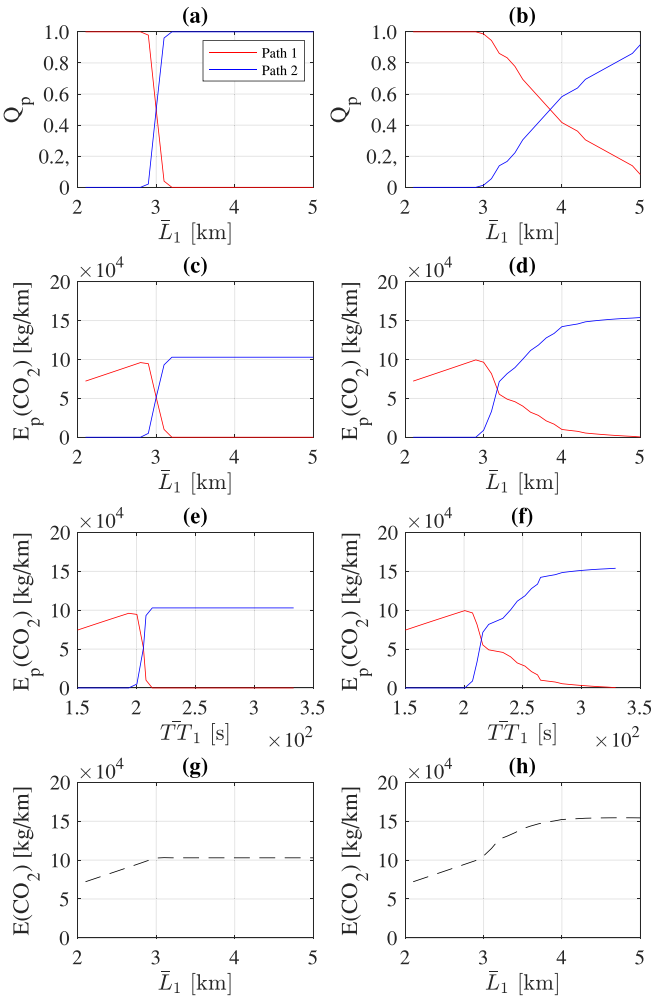

FIGURE 6. Same as in Figure 5, but for Scenarios 3 and 4. Panels (a), (c), (e), and (g) show the results for Scenario 3. Panels (b), (d), (f), and (h) show the results for Scenario 4.

Scenario 3 is that we include an additional internal path in region 3, which has a constant demand of 1 [veh/s]. This internal path increases the travel time of the second path $p_2 = \{134\}$ due to the speed homogeneity assumption of the MFD, acting as a potential bottleneck. Figure 6 (b), (d), (f) and (h) depict these results. We observe that thanks to the inclusion of this internal path in region 3, drivers start to switch from path $p_1 = \{124\}$ to $p_2 = \{134\}$ at a longer average travel distance $\bar{L}_1$ when compared to the previous Scenario 3. Until the point when drivers start to switch their paths, the total emissions of CO_2 increase linearly with $\bar{L}_1$. The maximum total emissions of CO_2 for the path $p_1 = \{124\}$ is larger than in the case of Scenario 3. This shows that not only the average travel distance of paths but also the interactions with demand from other OD pairs can influence the total path emissions of CO_2. In Scenario 3, we also observe that the linear decrease of $E_1(CO_2)$ for path $p_1 = \{124\}$, also results in a linear increase of $E_2(CO_2)$ for $p_2 = \{134\}$. However, this is not observed in the case of Scenario 4 between $\bar{L}_1 \sim 3 - 4$[kms] (see Figure 6 (d)) or

between the paths average travel times between 2000 and 2700 [s] (see Figure 6 (f)). When region 3 becomes more congested due to drivers traveling on $p_3 = \{3\}$, the accumulation of vehicles increases, leading to a decrease in the region's mean speed and an increase in the travel time for path $p_2 = \{134\}$. This changes the User Equilibrium conditions compared to Scenario 3, leading to the fact that a lower fraction of drivers switches from path $p_1 = \{124\}$ to path $p_2 = \{134\}$ as a function of $\overline{L}_1$ in Scenario 4 than in 3. The inclusion of an internal path in region 3 has a clear impact on the total network emissions of CO_2 as depicted in Figure 6 (h). The increase of congestion in the network reduces the mean speeds $\bar{v}$ which together with an increase in the travel production (i.e., the increase of $\overline{L}_1$) leads to an increase in the total network emissions of CO_2.

Figure 7 shows the evolution trend of the total exhaust emissions of carbon dioxide $E_3(CO_2)$ for the internal path $p\{3\}$, as a function of the average travel distance $\overline{L}_1$ and the average travel time $\overline{TT}_3$. For lower $\overline{L}_1$ values, no one chooses path $p_2 = \{134\}$ as all drivers choose to travel on path $p_1 = \{124\}$. Since the demand traveling on the internal path is constant, both the total exhaust emissions $E_3(CO_2)$ and the average travel time $\overline{TT}_3$ are also constant. This happens until drivers start switching from path $p_1 = \{124\}$ to $p_2 = \{134\}$, increasing the number of vehicles traveling in region 3, i.e., n_3. Thanks to the MFD assumption of speed homogeneity in the regions, an increase of the accumulation n_3 leads automatically to a reduction of the mean speed of all vehicles traveling in all paths in region 3. This naturally includes the internal path $p_3 = \{3\}$. The decrease of the mean speed $\bar{v}_3$ leads to an increase in the average travel time $\overline{TT}_3$ and of the total exhaust emissions $E_3(CO_2)$ as well. Following the discussion of Section IV-B, we also observe the linear increase of the total exhaust emissions $E_3(CO_2)$ of the internal path as a function of the average travel distance $\overline{L}_1$ and average travel time $\overline{TT}_3$. This relationship happens as long as the accumulation of vehicles in region 3 also increases. For larger values of $\overline{L}_1$, all drivers choose path $p_2 = \{134\}$. The accumulation n_3 remains constant as $\overline{L}_1$ increases, which leads to constant total exhaust emissions $E_3(CO_2)$ of the internal path.

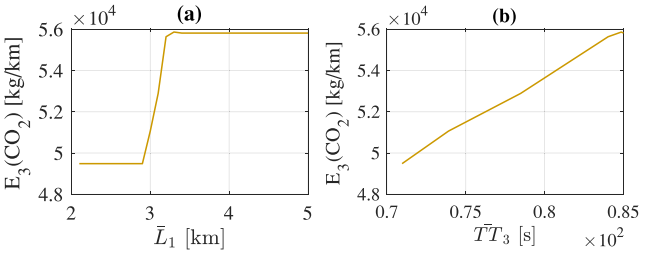

FIGURE 7. Evolution of the total CO_2 emissions of the internal path $p_3 = \{3\}$ as a function of the: (a) average travel distance $\overline{L}_1$ [km]; (b) path travel time $\overline{TT}_p^{OD}$. The results are depicted for Scenario 4.

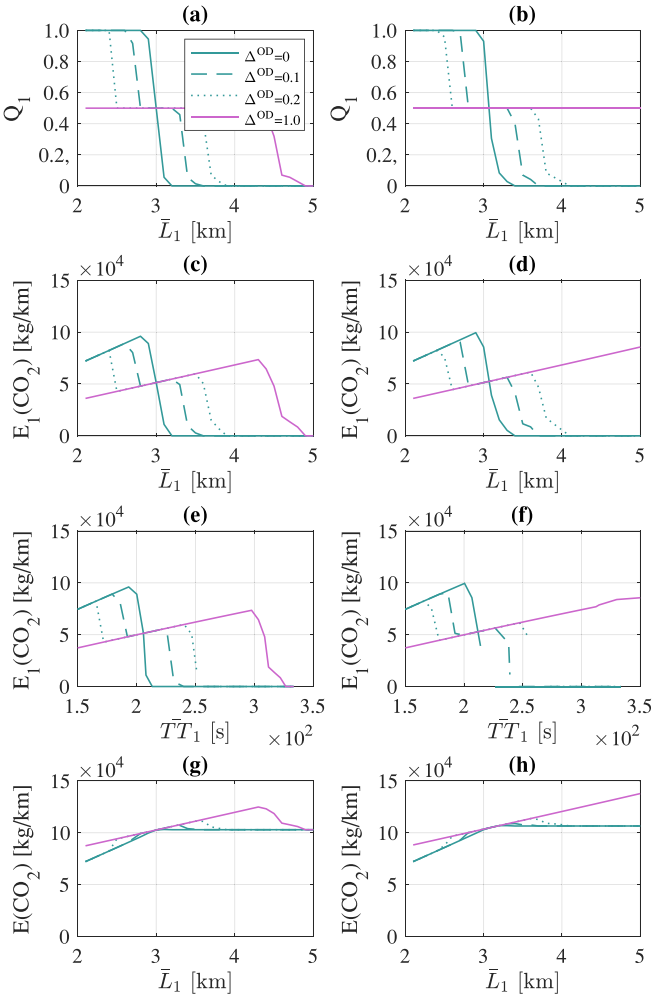

FIGURE 8. Same as in Figure 6, but for the Bounded Rational Deterministic User Equilibrium and Scenarios 5 and 6.

E. 4-REGION NETWORK UNDER BR-UE CONDITIONS

This subsection analyzes the results for Scenarios 5 and 6, tested on the 4-region network (Figure 2 (b)). Figure 8 depicts the results for these two scenarios, and the four settings of the indifference band Δ^{OD}: 0; 0.1; 0.2; and 1.0. The left panels refer to the results of Scenario 5, while the right panels refer to the results of Scenario 6. For simplicity, we only show the results for path $p_1 = \{124\}$ as the analysis for the other path is similar. Panels (a) and (b) show the evolution of the flows Q_p of path $p_1 = \{124\}$ as a function of the average travel distance $\overline{L}_1$ [km]. Panels (c) and (d), as well as (e) and (f), show the evolution of the total exhaust emissions $E_p(CO_2)$ of carbon dioxide of path $p_1 = \{124\}$ as a function of the average travel distance $\overline{L}_1$ [km] and average travel time $\overline{TT}_1$ [s], respectively. Panels (g) and (h) depict the evolution of the total network exhaust emissions $E(CO_2)$ as a function of the average travel distance $\overline{L}_1$ [km].

In Scenario 5, we calculated the Bounded Rational User Equilibrium conditions for all values of the average travel distances $\overline{L}_1$ [km] of path 1. Recall that we consider that drivers are indifferent towards any path as long as it is perceived as satisficing. For $\Delta^{OD} = 0$, we obtain similar results as the Deterministic User Equilibrium as depicted in

Figure 6. This is expected as for $\Delta^{OD} = 0$, only the path with the minimum travel time is perceived as satisficing, i.e., drivers are travel time minimizers. As Δ^{OD} increases, drivers start to perceive path $p_2 = \{134\}$ as satisficing also and start to switch to this path for lower $\overline{L}_1$ values. This has a natural influence on the total exhaust emissions of path $p_1 = \{124\}$, which start decreasing at lower values of $\overline{L}_1$ since drivers start to switch to the other path $p_2 = \{134\}$. On the other hand, as we increase the average travel distance $\overline{L}_1$, the total exhaust emissions of path $p_1 = \{124\}$ also increase linearly until all drivers start shifting to path $p_2 = \{134\}$. When $\Delta^{OD} = 1.0$, both paths are perceived as satisficing until $\overline{L}_1 \sim 4.3$ [kms]. In this case, the demand is equally split on both paths, and the total exhaust emissions $E_p(CO_2)$ increase linearly as a function of both the average travel distance $\overline{L}_1$ and average travel time $\overline{TT}_p$. As Δ^{OD} increases, the total network exhaust emissions $E(CO_2)$ increase as $\overline{L}_1$ does. This is because drivers have to travel a longer travel distance on path $p_1 = \{124\}$, i.e., an increase in the travel production leads to an increase in the total network exhaust emissions. This linear trend happens until all drivers start switching to the other path $p_2 = \{134\}$.

In Scenario 6, we also calculated the Bounded Rational User Equilibrium conditions as in Scenario 5. However, in this scenario, we also consider the internal path $p_3 = \{3\}$. The inclusion of this internal path acts as a bottleneck, which increases the travel time of path $p_2 = \{134\}$ as the accumulation in region 3 also increases. This changes the path choices of drivers traveling on the OD pair 14, and therefore the equilibrium dynamics of the network. For example, compared to Scenario 5, when $\Delta^{OD} = 1.0$ both paths $p_1 = \{124\}$ and $p_2 = \{134\}$ are now perceived as satisficing for all values of $\overline{L}_1$. The demand is then equally split on both paths. Given the path flow $Q_p = 0.5$, the total exhaust emissions of path $p_1 = \{124\}$ increases linearly as a function $\overline{L}_1$, as expected. This also leads to a linear increase of the total network exhaust emissions $E(CO_2)$, as the increase of $\overline{L}_1$ also increases the total travel production of the network.

F. DISCUSSION

All in all, we observe that in some cases there is a linear relationship between the total path emissions of CO_2 and the average travel distance or the average travel time. However, in more complex scenarios when there are interactions between different OD pairs, the traffic dynamics also play an important role in the relationship between the total path emissions of CO_2 and the average travel distance or the average travel time. Moreover, we can see how these different factors also affect the overall network emissions of CO_2. The most ecological-friendly paths in the regional network are not necessarily the ones with minimal average travel times or travel distances. Nevertheless, the linear trend observed between the total exhaust emissions of internal paths and the average travel time $\overline{TT}_p$ is a general result. This linear trend is a direct consequence of the speed homogeneity assumption of the MFD.

V. CHARACTERIZATION OF ECO-FRIENDLY PATHS IN A REAL TEST NETWORK

This section discusses the relationship between the total exhaust emissions of paths on regional networks and the average travel distance and travel time on a real urban network representing the city of Innsbruck (Austria). Figure 9 (a) depicts the test network. The map data was retrieved from OpenStreeMaps [46]. This network has 1992 nodes and 4448 links. We partition the network into four regions. This partitioning considers geographical features as discussed in [47]. The Inn river separates regions 2 and 3 from regions 1 and 4. The main railroad separates regions 1 and 4. Figure 9 (b) shows the production-MFD functions associated with each region. We also set a demand scenario consisting of 9 OD pairs, leading to 19 paths. The latter includes 15 regional paths and 4 internal paths. To calibrate the travel distances of these paths, we determine a synthetic set of trips in distance considering all possible trips between all potential origin and destination nodes in the urban network. Based on this set, we follow the methodology proposed by [32] to determine average travel distances per region and path. Figure 9 (c) shows the demand, defining the inflow of vehicles per second that travel on each of the OD pairs. We consider a total simulation period of $T = 6$ [hr]. We determine the Bounded Rational User Equilibrium conditions for different values of the indifference band Δ^{OD}: 0; 0.1; 0.2; and 0.5. The network achieves the equilibrium conditions when the Gap is inferior to a predefined threshold of 0.1. We set a maximum of 20 descent step iterations for the Method of Successive Averages. We also utilize an accumulation-based MFD model to mimic the traffic dynamics in the network.

Figure 10 shows the evolution of the regions' mean speeds $\overline{v}_r, \forall r = 1, \ldots, 4$ as a function of the simulation time t [hr]. The results are depicted for the different values of the indifference band. As Δ^{OD} increases, drivers perceive paths with longer travel distances as satisficing. This results in more congestion in the regions. A longer distance to be traveled in a region means that drivers require more time to complete their trips in the region as all vehicles travel at the same average speed. In this case, congestion lasts longer in the regions as Δ^{OD} increases. This can be observed in regions 1, 2, and 4 in Figure 10, where the mean speed decreases as Δ^{OD} increases. As drivers also choose paths with longer travel distances, this increases the total travel production in the network, leading to an increase in the total network exhaust emissions as the indifference level of drivers toward their path choices also increases. To show this effect, we determine the relative differences ϵ [%] between the total exhaust emissions of carbon dioxide of the network under Deterministic User Equilibrium conditions (i.e., equivalent to $\Delta^{OD} = 0$), E^{UE}, and under Bounded Rational User Equilibrium (BR-UE), E^{BRUE}:

$$\epsilon = \frac{E^{BRUE} - E^{UE}}{E^{UE}} \times 100\% \tag{9}$$

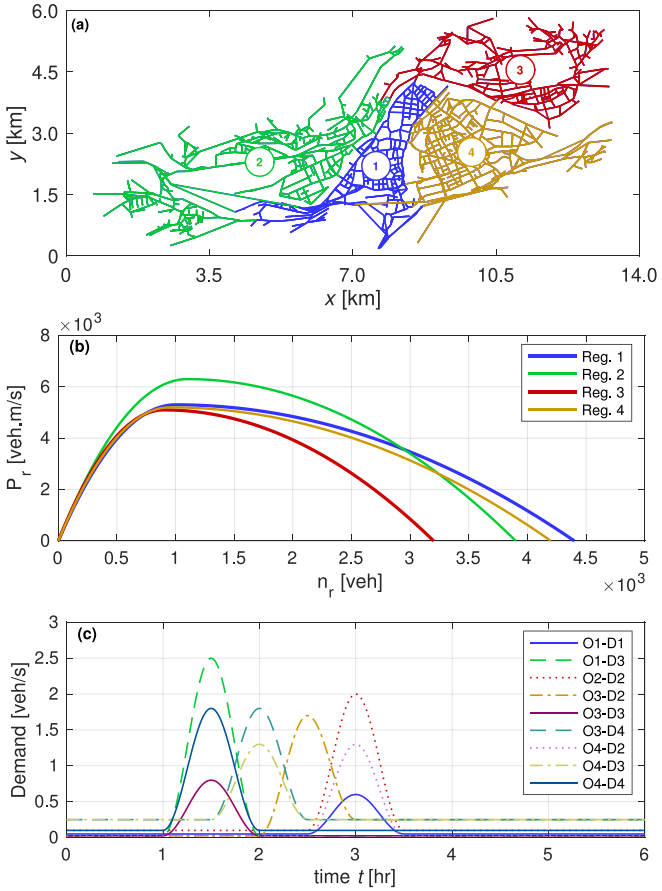

FIGURE 9. (a) Innsbruck network partitioned into four regions. (b) MFD functions. (c) Demand scenarios.

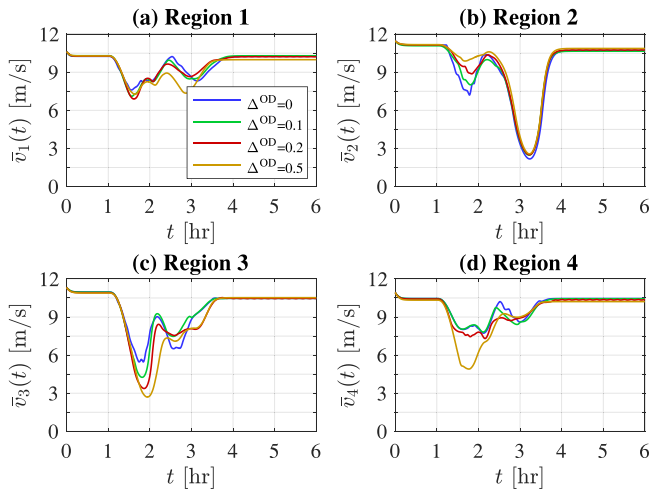

FIGURE 10. Evolution of the mean speed $\overline{v}_r, \forall r = 1, \ldots, 4$ [m/s] as a function of the simulation time t [hr]. The results are depicted for different levels of the indifference band $\Delta^{OD} = 0, 0.1, 0.2, 0.5$.

where the total network exhaust emissions of the BR-UE equilibrium correspond to the following settings of the indifference band Δ^{OD}: 0.1; 0.2; and 0.5.

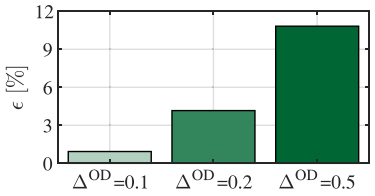

FIGURE 11. Relative differences ϵ [%] between the total network emissions of CO_2 related to the UE (i.e., $\Delta^{OD} = 0.0$), and the ones resulting from the BR-UE conditions for the three different values of the indifference band $\Delta^{OD} = 0.1, 0.2, 0.5$.

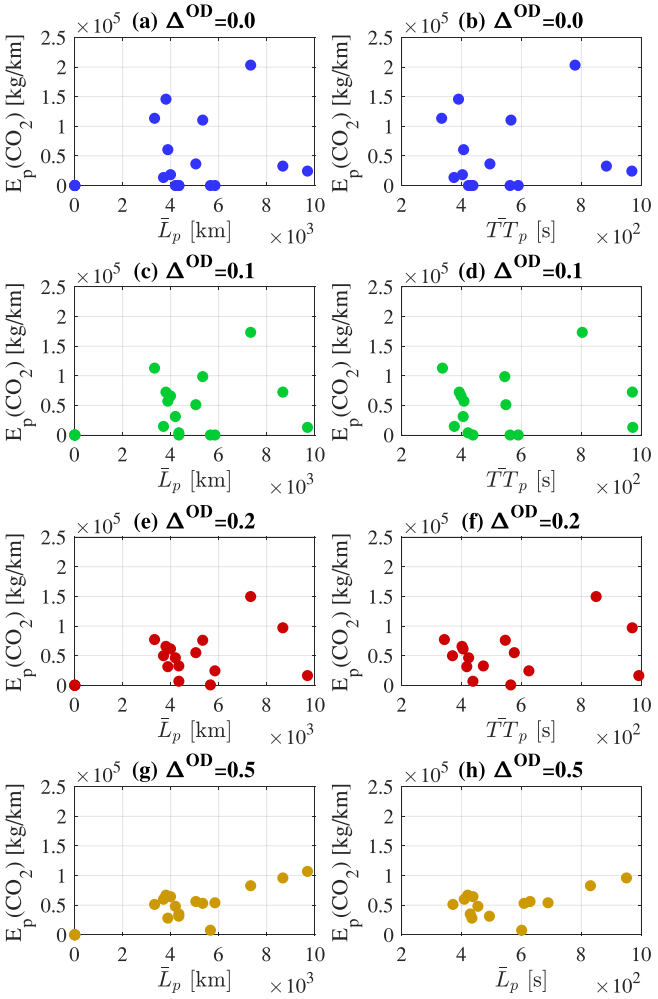

FIGURE 12. Total CO_2 emissions per path as a function of the average path travel distance $\overline{L}_p$ [km], and the average path travel time $\overline{TT}_p^{OD}$ [s]. The results are depicted for the Innsbruck network, and different levels of the indifference band $\Delta^{OD} = 0, 0.1, 0.2, 0.5$.

Figure 11 depicts the results of the relative differences ϵ [%]. As one can observe, when drivers are completely indifferent, i.e., $\Delta^{OD} = 0.5$, the total network exhaust emissions increase by $\sim$ 14% when compared to the Deterministic User Equilibrium conditions.

Figure 12 depicts the total exhaust emissions $E_p(CO_2)$ of carbon dioxide of all 15 regional paths as a function of the average travel distance $\overline{L}_p$ [km] and the average travel time $\overline{TT}_p$ [s]. Each point represents the total exhaust emissions

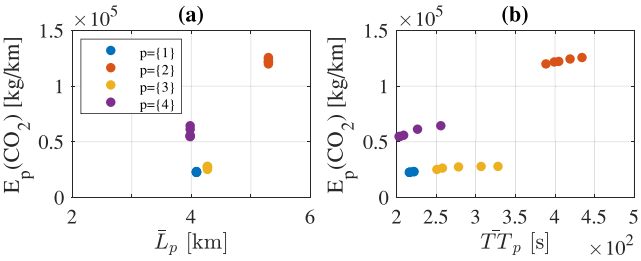

FIGURE 13. Same as in Figure 7, but for the four internal paths. The results are depicted for the same four values of the indifference band.

$E_p(CO_2)$ of each path. The results are depicted for the four settings of the indifference band Δ^{OD}, which represent different traffic dynamics in the network as shown in Figure 10. As one can observe, there is no clear relationship between the total exhaust emissions $E_p(CO_2)$ and the average travel distance of paths $\overline{L}_p$ or the average travel time $\overline{TT}_p$, as the complex traffic dynamics play an important role on the total exhaust emissions.

Figure 13 shows the total exhaust emissions $E_p(CO_2)$ of the 4 internal paths as a function of the average travel distance $\overline{L}_p$ [km] and the average travel time $\overline{TT}_p$ [s]. Each point represents the total exhaust emissions of each internal path for each setting of Δ^{OD}. For each internal path, the point found more to the left corresponds to $\Delta^{OD} = 0$, while the point that is the most to the right corresponds to $\Delta^{OD} = 0.5$. As one can observe, there is a linear trend between $E_p(CO_2)$ and the average path travel time $\overline{TT}_p$. As drivers choose paths with longer travel distances in the regions as Δ^{OD} increases, the total travel production in the region also increases and therefore leads to an increase in the $E_p(CO_2)$ (see Eq. (7)).

VI. CONCLUSION

In this paper, we investigate the relationship between the total emissions of CO_2 ($E_p(CO_2)$) of paths in regional networks and their average travel distance or travel time. We recall that paths on regional networks present different features than trips in urban networks. In particular, there are three main variables that explain such differences, and lead to the relationships or lack thereof between total exhaust emissions and travel distance or travel time shown and discussed in this paper: (i) the heterogeneity of travel distances of all paths that travel in each region; (ii) the speed homogeneity assumption of the MFD, which together with the heterogeneity of travel distances of all paths in one region have a significant influence in the modeled network dynamics; and (iii) the complex interactions between the demand traveling on different OD pairs. We conducted tests on two toy networks composed of 1 and 4 regions respectively, and a real urban network representing the city of Innsbruck (Austria). We utilized an accumulation-based MFD model to mimic the traffic dynamics and determined the CO_2 path emissions using COPERT.

The results of this paper clearly show that:

- There is a clear relationship between the distance traveled (or the travel time) in a region and the traveling exhaust emissions. Thanks to the speed homogeneity assumption of the MFD, a longer travel distance in the region requires a longer travel time for drivers to complete their trips. This increases the congestion in the region, leading to higher travel exhaust emissions.
- Internal paths show a clear relationship between travel emissions and travel times or travel distances thanks to the MFD speed homogeneity assumption.
- There is no clear relationship between the path travel distance (or travel time) and the traveling exhaust emissions. We verify the existence of a relationship only under very simplified scenarios. However, in more realistic scenarios where the number of OD pairs is larger, the interactions between the demand traveling on different OD pairs and the traffic dynamics become more complex. Therefore at the path level, there is no clear relationship between the distance traveled (or the travel time) in a region and the traveling exhaust emissions due to the complex dynamics.

The findings discussed in this paper provide important guidance for designing green-routing strategies using the MFD-based traffic models, with control systems that monitor travel exhaust emissions for example in downtown regions of cities (see, e.g., [48]). Following the insights of this paper, if only a single region is controlled, then the controlled should penalize paths crossing this region that have longer travel distances. If multiple downtown regions are monitored, then the controller should penalize paths not only with longer travel distances but also that travel through regions that tend to be more congested. All in all, these insights are important for the adoption of eco-routing strategies linked with tolling systems or perimeter control schemes [49]. In the follow-up of this paper, we plan to: (i) investigate the relationship between the Dynamic System Optimum in regional networks, in terms of minimizing the total travel time and the total exhaust emissions of the system; and (ii) develop a Dynamic Social Optimum route guidance system with perimeter control feedback that monitors the travel exhaust emissions. Such systems could bring significant benefits compared to the current user equilibrium conditions [50]. Furthermore, we note that the partitioning of urban networks into regional (or aggregated) networks for applying the aggregated traffic models based on the MFD is still a question of research in the literature. Several efforts have been made in the last years in this direction. As the authors in [30] mentioned, the partitioning/clustering of urban networks should yield, on one hand, regions that are topologically well-separated, compact, and fully connected, while on the other hand, the traffic conditions should be approximately homogeneous in each one of the regions. In this paper, we partitioned the Innsbruck network taking into account geographical features [30]. As a future research direction, more efforts should be put into

developing approaches to partition urban networks while accounting for the appropriate topological features and the homogeneity of traffic conditions.

ACKNOWLEDGMENT

The authors thank the reviewers for their comments and suggestions which have much improved the quality of our paper. They thank Gabriel Tilg for help on gathering and correcting the network of Innsbruck from OpenStreetMaps.

REFERENCES

[1] G. H. Tzeng and C.-H. Chen, "Multiobjective decision making for traffic assignment," *IEEE Trans. Eng. Manag.*, vol. 40, no. 2, pp. 180–187, May 1993.

[2] L. Rilett and C. Benedek, "Traffic assignment under environmental and equity objectives," *Transp. Res. Rec.*, vol. 1443, pp. 92–99, Oct. 1994.

[3] C. M. Benedek and L. R. Rilett, "Equitable traffic assignment with environmental cost functions," *J. Transp. Eng.*, vol. 124, no. 1, pp. 16–22, 1998.

[4] A. Nagurney, "Congested urban transportation networks and emission paradoxes," *Transp. Res. D, Transp. Environ.*, vol. 5, no. 2, pp. 145–151, 2000.

[5] A. Nagurney and J. Dong, "A multiclass, multicriteria traffic network equilibrium model with elastic demand," *Transp. Res. B, Methodol.*, vol. 36, no. 5, pp. 445–469, 2002.

[6] S. Sugawara and D. A. Niemeier, "How much can vehicle emissions be reduced? Exploratory analysis of an upper boundary using an emissions-optimized trip assignment," *Transp. Res. Rec.*, vol. 1815, no. 1, pp. 29–37, 2002.

[7] Y. Yin and S. Lawphongpanich, "Internalizing emission externality on road networks," *Transp. Res. D, Transp. Environ.*, vol. 11, no. 4, pp. 292–301, 2006.

[8] S. Sharma and T. V. Mathew, "Multiobjective network design for emission and travel-time trade-off for a sustainable large urban transportation network," *Environ. Plan. B, Plan. Design*, vol. 38, no. 3, pp. 520–538, 2011.

[9] A. Chen, S. Pravinvongvuth, X. Xu, S. Ryu, and P. Chootinan, "Examining the scaling effect and overlapping problem in logit-based stochastic user equilibrium models," *Transp. Res. A*, vol. 46, pp. 1343–1358, Oct. 2012.

[10] H. M. A. Aziz and S. V. Ukkusuri, "Integration of environmental objectives in a system optimal dynamic traffic assignment model," *Comput.-Aided Civil Infrastruct. Eng.*, vol. 27, no. 7, pp. 494–511, 2012.

[11] Y. M. Nie and Q. Li, "An eco-routing model considering microscopic vehicle operating conditions," *Transp. Res. B, Methodol.*, vol. 55, pp. 154–170, 2013.

[12] K. Ahn and H. A. Rakha, "Network-wide impacts of eco-routing strategies: A large-scale case study," *Transp. Res. D, Transp. Environ.*, vol. 25, pp. 119–130, Dec. 2013.

[13] L. Guo, S. Huang, and A. W. Sadek, "An evaluation of environmental benefits of time-dependent green routing in the greater Buffalo–Niagara region," *J. Intell. Transp. Syst.*, vol. 17, no. 1, pp. 18–30, 2013.

[14] C.-C. Lu, J. Liu, Y. Qu, S. Peeta, N. M. Rouphail, and X. Zhou, "Eco-system optimal time-dependent flow assignment in a congested network," *Transp. Res. B, Methodol.*, vol. 94, pp. 217–239, Dec. 2016.

[15] J. Long, J. Chen, W. Y. Szeto, and Q. Shi, "Link-based system optimum dynamic traffic assignment problems with environmental objectives," *Transp. Res. D, Transp. Environ.*, vol. 60, pp. 56–75, May 2018.

[16] W. Zeng, T. Miwa, and T. Morikawa, "Eco-routing problem considering fuel consumption and probabilistic travel time budget," *Transp. Res. D, Transp. Environ.*, vol. 78, Jan. 2020, Art. no. 102219.

[17] C. F. Daganzo, "Urban gridlock: Macroscopic modeling and mitigation approaches," *Transp. Res. B, Methodol.*, vol. 41, pp. 49–62, Jan. 2007.

[18] Y. Wang, W. Y. Szeto, K. Han, and T. L. Friesz, "Dynamic traffic assignment: A review of the methodological advances for environmentally sustainable road transportation applications," *Transp. Res. B, Methodol.*, vol. 111, pp. 370–394, May 2018.

[19] J. Marques, S. Batista, M. Menendez, E. Macedo, and M. C. Coelho, "From aggregated traffic models to emissions quantification: Connecting the missing dots," *Transp. Res. Procedia*, vol. 69, pp. 568–575, Feb. 2023.

[20] K. Ahn and H. Rakha, "The effects of route choice decisions on vehicle energy consumption and emissions," *Transp. Res. D, Transp. Environ.*, vol. 13, no. 3, pp. 151–167, 2008.

[21] K. Boriboonsomsin, J. Dean, and M. Barth, "Examination of attributes and value of ecologically friendly route choices," *Transp. Res. Rec.*, vol. 2427, no. 1, pp. 13–25, 2014.

[22] H. A. Aziz and S. V. Ukkusuri, "Exploring the trade-off between greenhouse gas emissions and travel time in daily travel decisions: Route and departure time choices," *Transp. Res. D, Transp. Environ.*, vol. 32, pp. 334–353, Oct. 2014.

[23] I. D. Vlieger, D. D. Keukeleere, and J. Kretzschmar, "Environmental effects of driving behaviour and congestion related to passenger cars," *Atmos. Environ.*, vol. 34, no. 27, pp. 4649–4655, 2000.

[24] M. Barth, K. Boriboonsomsin, and A. Vu, "Environmentally-friendly navigation," in *Proc. IEEE Intell. Transp. Syst. Conf.*, 2007, pp. 684–689.

[25] H. C. Frey, K. Zhang, and N. M. Rouphail, "Fuel use and emissions comparisons for alternative routes, time of day, road grade, and vehicles based on in-use measurements," *Environ. Sci. Technol.*, vol. 42, no. 7, pp. 2483–2489, 2008.

[26] J. Bandeira, T. G. Almeida, A. J. Khattak, N. M. Rouphail, and M. C. Coelho, "Generating emissions information for route selection: Experimental monitoring and routes characterization," *J. Intell. Transp. Syst.*, vol. 17, no. 1, pp. 3–17, 2013.

[27] J. M. Bandeira et al., "Empirical assessment of route choice impact on emissions over different road types, traffic demands, and driving scenarios," *Int. J. Sustain. Transp.*, vol. 10, no. 3, pp. 271–283, 2016.

[28] S. Batista, M. Seppecher, and L. Leclercq, "Identification and characterizing of the prevailing paths on a urban network for MFD-based applications," *Transp. Res. C, Emerg. Technol.*, vol. 127, Jun. 2021, Art. no. 102953.

[29] C. Lopez, L. Leclercq, P. Krishnakumari, N. Chiabaut, and H. van Lint, "Revealing the day-to-day regularity of urban congestion patterns with 3D speed maps," *Sci. Rep.*, vol. 7, Oct. 2017, Art. no. 14029.

[30] S. F. A. Batista, C. Lopez, and M. Menéndez, "On the partitioning of urban networks for MFD-based applications using Gaussian mixture models," in *Proc. 7th Int. Conf. Models Technol. Intell. Transp. Syst. (MT-ITS)*, 2021, pp. 1–6.

[31] M. Ameli, M. S. S. Faradonbeh, J.-P. Lebacque, H. Abouee-Mehrizi, and L. Leclercq, "Departure time choice models in urban transportation systems based on mean field games," *Transp. Sci.*, vol. 56, no. 6, pp. 1483–1504, 2022.

[32] S. F. A. Batista, L. Leclercq, and N. Geroliminis, "Estimation of regional trip length distributions for the calibration of the aggregated network traffic models," *Transp. Res. B, Methodol.*, vol. 122, pp. 192–217, Apr. 2019.

[33] M. Ameli, J.-P. Lebacque, and L. Leclercq, "Simulation-based dynamic traffic assignment: Meta-heuristic solution methods with parallel computing," *Comput.-Aided Civil Infrastruct. Eng.*, vol. 35, no. 10, pp. 1047–1062, 2020.

[34] G. Mariotte, L. Leclercq, and J. A. Laval, "Macroscopic urban dynamics: Analytical and numerical comparisons of existing models," *Transp. Res. B, Methodol.*, vol. 101, pp. 245–267, Jul. 2017.

[35] L. Ntziachristos, D. Gkatzoflias, C. Kouridis, and Z. Samaras, "COPERT: A European road transport emission inventory model," in *Information Technologies in Environmental Engineering* (Environmental Science and Engineering), I. N. Athanasiadis, A. E. Rizzoli, P. A. Mitkas, J. M. Gómez, Eds, Berlin, Germany: Springer, 2009, [Online]. Available: https://doi.org/10.1007/978-3-540-88351-7_37

[36] S. F. A. Batista and L. Leclercq, "Regional dynamic traffic assignment framework for MFD multi-regions models," *Transp. Sci.*, vol. 53, no. 6, pp. 1563–1590, 2019.

[37] H. A. Simon, *A Behavioral Model of Rational Choice*. New York, NY, USA: Wiley, 1957.

[38] H. Mahmassani, J. C. Williams, and R. Herman, "Investigation of network-level traffic flow relationships: Some simulation results," *Transp. Res. Rec. J. Transp. Res. Board*, vol. 971, pp. 121–130, Jan. 1984.

[39] M. Ameli, J.-P. Lebacque, and L. Leclercq, "Improving traffic network performance with road banning strategy: A simulation approach comparing user equilibrium and system optimum," *Simulat. Model. Pract. Theory*, vol. 99, Feb. 2020, Art. no. 101995.
[40] S. F. A. Batista, C.-L. Zhao, and L. Leclercq, "Effects of users' bounded rationality on a traffic network performance: A simulation study," *J. Adv. Transp.*, vol. 2018, Sep. 2018, Art. no. 9876598.
[41] S. Batista and L. Leclercq, "Regional dynamic traffic assignment with bounded rational drivers as a tool for assessing the emissions in large metropolitan areas," *Transp. Res. Interdiscip. Perspect.*, vol. 8, Nov. 2020, Art. no. 100248.
[42] M. Ameli, J.-P. Lebacque, and L. Leclercq, "Cross-comparison of convergence algorithms to solve trip-based dynamic traffic assignment problems," *Comput.-Aided Civil Infrastruct. Eng.*, vol. 35, no. 3, pp. 219–240, 2020.
[43] D. Lejri, A. Can, N. Schiper, and L. Leclercq, "Accounting for traffic speed dynamics when calculating COPERT and PHEM pollutant emissions at the urban scale," *Transp. Res. D, Transp. Environ.*, vol. 63, pp. 588–603, Aug. 2018.
[44] D. Lejri and L. Leclercq, "Are average speed emission functions scale-free?" *Atmos. Environ.*, vol. 224, Mar. 2020, Art. no. 117324.
[45] D. Ingole, G. Mariotte, and L. Leclercq, "Perimeter gating control and citywide dynamic user equilibrium: A macroscopic modeling framework," *Transp. Res. C, Emerg. Technol.*, vol. 111, pp. 22–49, Feb. 2020.
[46] "OpenStreetMap contributors." Innsbruck Dump. 2020. [Online]. Available: https://planet.osm.org
[47] S. Batista, G. Tilg, and M. Menéndez, "Exploring the potential of aggregated traffic models for estimating network-wide emissions," *Transp. Res. D, Transp. Environ.*, vol. 109, Aug. 2022, Art. no. 103354.
[48] D. Ingole, G. Mariotte, and L. Leclercq, "Minimizing network-wide emissions by optimal routing through inner-city gating," *Transp. Res. D, Transp. Environ.*, vol. 86, Sep. 2020, Art. no. 102411.
[49] K. Yang, M. Menendez, and N. Zheng, "Heterogeneity aware urban traffic control in a connected vehicle environment: A joint framework for congestion pricing and perimeter control," *Transp. Res. C, Emerg. Technol.*, vol. 105, pp. 439–455, Aug. 2019.
[50] A. Belov, K. Mattas, M. Makridis, M. Menendez, and B. Ciuffo, "A microsimulation based analysis of the price of anarchy in traffic routing: The enhanced Braess network case," *J. Intell. Transp. Syst.*, vol. 26, no. 4, pp. 448–460, 2022.

SÉRGIO F. A. BATISTA graduated in physics and applied mathematics from the Faculty of Sciences, University of Porto, Portugal. In 2015, he joined the Horizon 2020 ERC Project MAGnUM and received the Ph.D. degree in civil engineering (focusing on transportation) from the University of Lyon, France, in 2018. He is currently a Research Faculty with New York University Abu Dhabi, UAE. He has authored more than ten papers, and several conference papers and actively acts as a reviewer for more than ten scientific journals. His main research interests include traffic flow theory, network modeling, and decarbonization of transportation, and adaptation to climate change.

MOSTAFA AMELI received the B.Sc. and M.Sc. degrees (with Distinction) in industrial engineering from the University of Tehran, Tehran, Iran, in 2014 and 2016, respectively, and the second M.Sc. degree in mechanical engineering from Arts et Métiers ParisTech, Paris, France, in 2016. He joined the Horizon 2020 ERC Project, MAGnUM, in 2016 and received the Ph.D. degree from University Paris-Est, IFSTTAR (The French Institute of Science and Technology devoted to Transport, Planning, and Networks), Paris, and the University of Lyon, Lyon, France, in 2019. He is currently an Assistant Professor of Applied Mathematics, Computer Science, and Transportation Science with the Transportation Engineering and Computer Science Lab (GRETTIA), Université Gustave Eiffel, Paris. Since 2022, he has been a Research Affiliate with the Department of Electrical Engineering and Computer Sciences, University of California at Berkeley, Berkeley, CA, USA. His research interest lies at the intersection of operations research and computer science, especially with applications in transportation management systems.

MÓNICA MENÉNDEZ (Member, IEEE) received the dual B.S. degree (*summa cum laude*) in civil and architectural engineering from the University of Miami, Coral Gables, FL, USA, in 2002, and the M.S. and Ph.D. degrees (focusing on transportation) from the University of California at Berkeley, Berkeley, CA, USA, in 2003 and 2006, respectively. She is the Associate Dean of Engineering for Graduate Programs and a Professor of Civil and Urban Engineering with New York University Abu Dhabi (NYUAD); as well as a Global Network Professor of Civil and Urban Engineering with the Tandon School of Engineering, New York University. She is also the Director of the NYUAD Research Center for Interacting Urban Networks (CITIES). Before joining NYUAD, she was the Director of the Research Group Traffic Engineering, ETH Zurich; and prior to that, a Management Consultant with Bain & Company. She has authored over 90 journal articles and over 200 conference contributions and technical reports in the area of transportation and is a member of multiple editorial boards for top journals in the field. Her research interests include multimodal transportation systems paying special attention to new technologies and information sources.